An Image Reconstruction algorithm for a dual head GAGG(Ce)-based compact 3D scanning setup

Aditya Garg

1 Introduction

Positron Emission Tomography (PET) is a medical imaging method that employs radioactive tracers emitting positrons to detect changes in metabolic process. PET employs gamma ray detectors that operate together to detect gamma rays emitted in the annihilation reaction that the positrons undergo. A GAGG(Ce) based dual head PET scanning setup was presented in [1] . In this document, we aim to devise an algorithm for Image reconstruction for the detector setup presented in the paper [1].

2 Setup

The detector setup comprises of two planar detectors employing a GAGG(Ce) crystal coupled with a Position Sensitive Photomultiplier Tube(PSPMT), placed facing each other at a separation of 40 cm from each other. Each detector has dimensions of 5 cm x 5 cm.

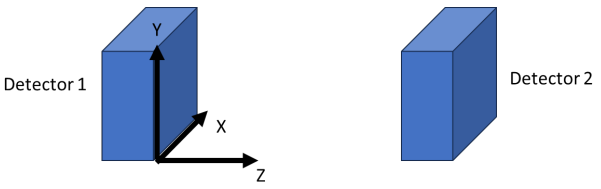

Figure 1: Depiction of the detector setup

The setup records x and y co-ordinates of photons detected at Detector 1(D1) (x_1, y_1) and Detector 2(D2) (x_2, y_2) sufficiently close in time.

3 Data Description

Three datasets were recorded with the initial setup by placing a ^{22}Na source at the positions (2.5 cm,2.5 cm,20 cm) [Dataset-A], (1.5 cm,2.5 cm,20 cm) [Dataset-B] and, (0.5 cm,2.5 cm,20 cm) [Dataset-C] recording (x_1, y_1) and (x_2, y_2)

4 Algorithm

The aim of the image reconstruction in the sense of this report is to determine to a sufficient accuracy the position of any radioactive material placed in the field of view of the setup.

4.1 An Initial Guess

The physics of the problem suggests a simple yet sufficiently efficient approach towards an estimate of the position of the radioactive material. Since the emitted photons in an electron positron annihilation travel in a straight line, taking the intersection of such straight lines should point to the location of annihilation and hence the location of the radioactive compound can be determined.

4.2 A more dicrete algorithm

Since we have an initial guess that is sufficiently accurate, we work with an iterative algorithm to improve on this estimate. We improvise the algorithm presented in [4] for our current setup.

4.2.1 Maximum Likelihood Expectation Maximization

The Maximum Likelihood Expectation Maximization (MLEM), first presented in [2], is an iterative algorithm to compute maximum likelihood estimates for an exponential family prior. The EM algorithm can be applied to an exponential family of the form

$$f(x|\Phi) = b(x)\exp(\Phi t(x)^T)/a(\Phi). \quad (1)$$

Given this form the EM algorithm can be proceeded in the following two steps applied iteratively.

- E-step: Estimate complete sufficient statistics t(x) by finding
$$t^{(p)} = E(t(x)|y, \Phi^{(p)}) \quad (2)$$
- M-step: Determine $\Phi^{(p+1)}$ as the solution of
$$E[t(x)|\Phi] = t^{(p)} \quad (3)$$

4.2.2 Setting up for an MLEM algorithm

Let $\lambda(x, y, z)$ represent the distribution of the source at the location (x,y,z). We wish to estimate lambda in our field of view(FOV). We divide our FOV into blocks of fixed size and indexed by $b = 1, 2, 3, 4, \ldots$. We also pair up detector slices with each other and index a pair of detectors on opposite detector pairs by d=1,2,3,4,5,..... . Let $n^*(d)$ represent the total number of coincidences detected by a detector pair and let p(b,d) represent the probability that a source located inside block b is detected by detector pair d. We denote by $\lambda(b)$ the integral of $\lambda(x, y, z)$ on the block b. Let n(b,d) represent the number of emissions in box b detected in tube d.

In our discretized model, where we have our FOV divided into discrete voxels, calculating $\lambda(b)$ for all b is our aim. We assume that n(b,d) are independent poisson variables with mean

$$E[n(b, d)] = \lambda(b, d) = \lambda(b)p(b, d) \quad (4)$$

. Thus,

$$P[n(b, d) = k] = e^{-\lambda(b,d)}\frac{\lambda(b, d)^k}{k!}. \quad (5)$$

Thus, the likelihood function is given by

$$L(\lambda) = P(n^*|\lambda) = \sum_A \prod_{b,\,d} e^{(-\lambda(b,d)\frac{\lambda(b,d)^{n(b,d)}}{n(b,d)!})} \quad (6)$$

where n^* represents our observed dataset.Note that $n^*(d) = \sum_{b=1}^{B} n(b, d)$ for d=1,2,3,4.,D and $n(b) = \sum_{d=1}^{D} n(b, d)$

4.2.3 MLEM for our setup

We have our E-step as

$$E[n(b)|\lambda] = E\left[\sum_d n(b, d)|\lambda\right] = \sum_d \frac{n^*(d)\lambda(b, d)}{\sum_{b'}\lambda(b')p(b', d)} \quad (7)$$

Then the M-step is given as

$$E[n(b)|\lambda^{new}] = \sum_d \frac{n^*(d)\lambda^{(old)}(b, d)}{\sum_b'\lambda^{(old)}(b')p(b', d)} \quad (8)$$

$$\lambda^{(new)}(b) = \sum_d \frac{n^*(d)\lambda^{(old)}(b, d)}{\sum_b'\lambda^{(old)}(b')p(b', d)} \quad (9)$$

$$= \sum_d \frac{n^*(d)\lambda^{(old)}(b)p(b, d)}{\sum_b'\lambda^{(old)}(b')p(b', d)} \quad (10)$$

$$= \lambda^{(old)}(b)\sum_d \frac{n^*(d)p(b, d)}{\sum_b'\lambda^{(old)}(b')p(b', d)} \quad (11)$$

Thus finally we obtain our iterative algorithm as,

$$\lambda^{(new)}(b) = \lambda^{(old)}(b)\sum_d \frac{n^*(d)p(b, d)}{\sum_b'\lambda^{(old)}(b')p(b', d)} \quad (12)$$

The algorithm intrinsically depends on the choice of p(b,d) i.e. the choice of the probability model. In the current setup, we use solid angles to estimate p(b,d). We take

$$p(b, d) = \frac{\Omega}{4\pi} \quad (13)$$

where Ω is the solid angle projected by the farther located detector element in the detector pair d at the center of the block b.

5 Results for the Initial Setup

The results of the computations for different datasets using the line intersection algorithm and the MLEM algorithm are presented below. The data suggests that the MLEM algorithm significantly reduces the size of the confidence interval for the Z coordinate whereas there is little fluctuations to both the mean and standard deviation of the X and Y coordinates. The fluctuations in the standard deviation can be attributed to the discretization introduced to carry out MLEM. The discretization although does not affect the precision in the Z-coordinate significantly, but since the length used for discretizing is comparable to the initial standard deviation of the intersection algorithm, such fluctuations are seen.

X-coordinate	Mean	Std Dev
Intersection Estimate	25.0499	2.1889
Iteration 1	25.5084	2.0586
Iteration 2	25.3443	1.8658
Iteration 3	25.0627	1.8216
Iteration 4	25.1209	2.0841
Iteration 5	25.7765	1.9303

Y-coordinate	Mean	Std Dev
Intersection Estimate	25.2197	2.0732
Iteration 1	25.0882	2.1907
Iteration 2	25.1257	2.1890
Iteration 3	25.2703	2.0853
Iteration 4	25.2308	2.2493
Iteration 5	25.1809	2.2208

Z-coordinate	Mean	Std Dev
Intersection Estimate	199.494	26.6586
Iteration 1	203.387	22.2398
Iteration 2	201.836	18.2534
Iteration 3	200.994	15.4486
Iteration 4	202.880	14.0447
Iteration 5	202.455	12.4729

Table 1: Results for Dataset-A (in mm)

X-coordinate	Mean	Std Dev
Intersection Estimate	15.5091	2.0762
Iteration 1	15.5057	2.0995
Iteration 2	15.7513	2.2619
Iteration 3	15.7556	2.2178
Iteration 4	15.9337	2.3283
Iteration 5	15.8636	2.1999

Y-coordinate	Mean	Std Dev
Intersection Estimate	25.3386	2.0932
Iteration 1	25.3557	1.9527
Iteration 2	25.3615	1.9069
Iteration 3	25.3296	1.9179
Iteration 4	25.2992	2.0201
Iteration 5	25.3103	2.0384

Z-coordinate	Mean	Std Dev
Intersection Estimate	188.672	31.2821
Iteration 1	190.651	24.2279
Iteration 2	191.787	20.6754
Iteration 3	192.146	18.2864
Iteration 4	193.425	16.3954
Iteration 5	194.047	14.8464

Table 2: Results for Dataset-B (in mm)

X-coordinate	Mean	Std Dev
Intersection Estimate	6.1282	1.6044
Iteration 1	6.3628	1.7137
Iteration 2	6.4152	1.7939
Iteration 3	6.3444	1.8533
Iteration 4	6.4229	1.9436
Iteration 5	6.4552	1.9392

Y-coordinate	Mean	Std Dev
Intersection Estimate	25.7011	2.2046
Iteration 1	25.6956	1.9964
Iteration 2	25.7096	1.8144
Iteration 3	25.7596	1.8769
Iteration 4	25.695.0	1.9893
Iteration 5	25.6638	1.9783

Z-coordinate	Mean	Std Dev
Intersection Estimate	176.314	30.5878
Iteration 1	179.672	25.2297
Iteration 2	181.290	21.6855
Iteration 3	182.602	20.8703
Iteration 4	184.966	20.0662
Iteration 5	184.745	19.6384

Table 3: Results for Dataset-C (in mm)

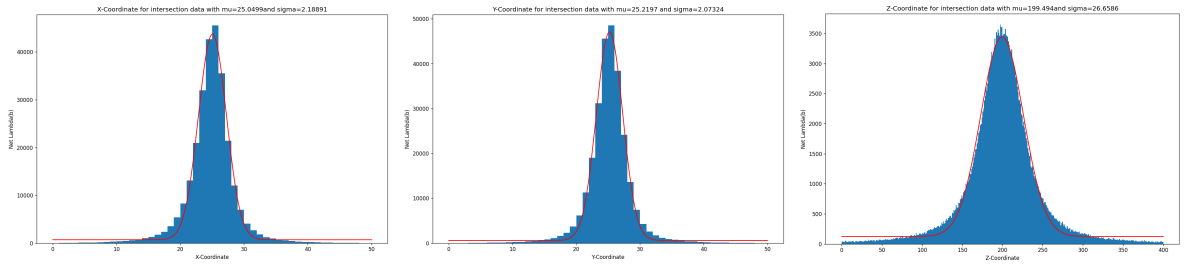

Figure 2: Intersection plots for Dataset-A

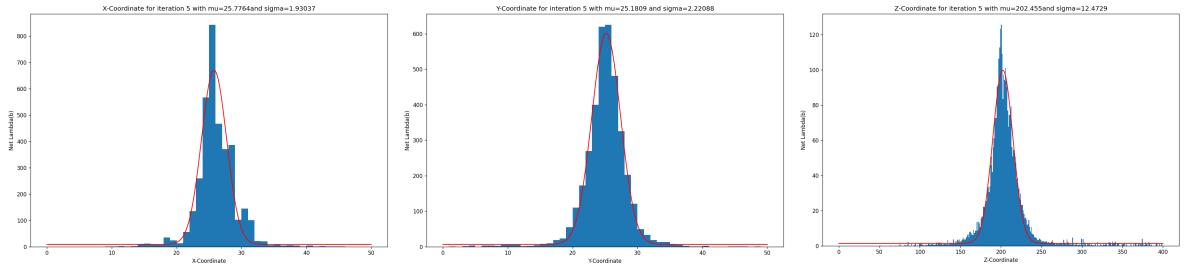

Figure 3: MLEM Iteration 5 plots for Dataset-A

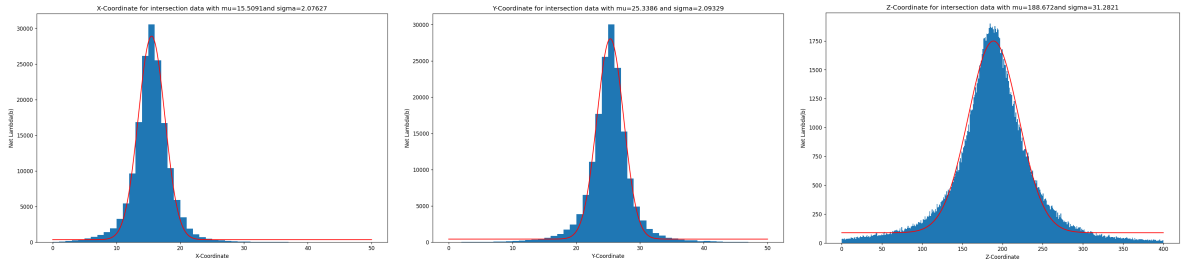

Figure 4: Intersection plots for Dataset-B

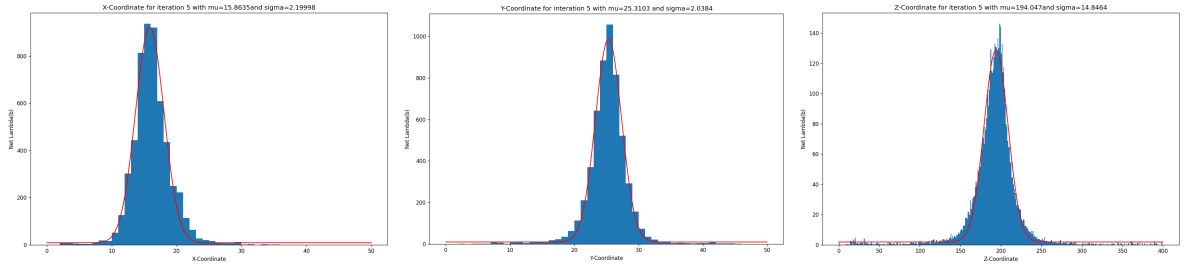

Figure 5: MLEM Iteration 5 plots for Dataset-B

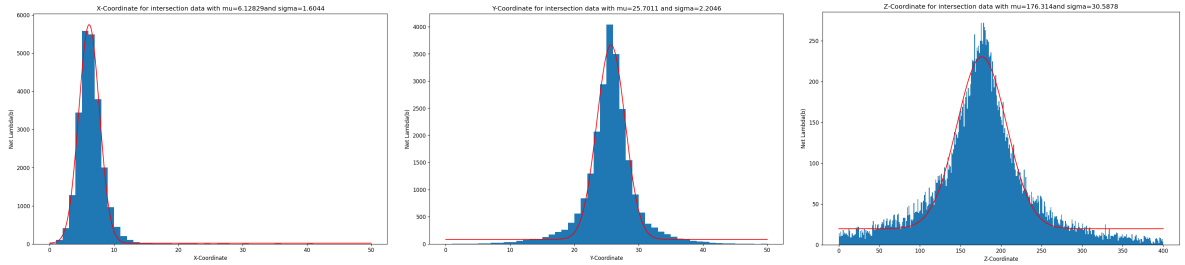

Figure 6: Intersection plots for Dataset-C

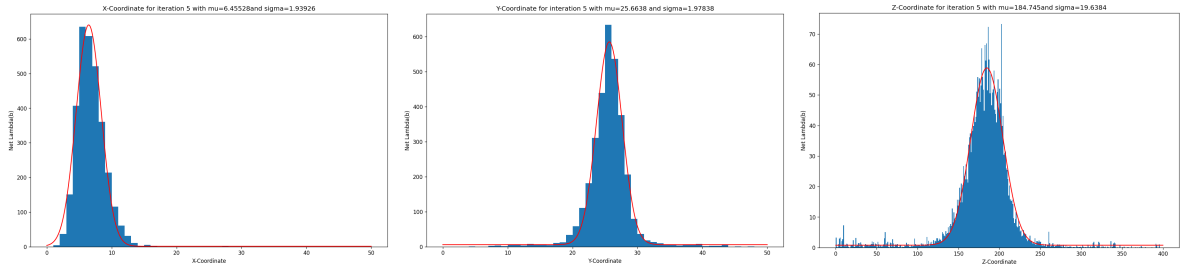

Figure 7: MLEM Iteration 5 plots for Dataset-C

6 Proposed Setup

The results from the initial setup suggest a significantly low precision along z direction. The low precision can be attributed to the comparatively large distance between the detector plates (i.e. 40 cm). So we propose a new setup employing four detectors placed so that their field of view is perpendicular to each other. In an ideal situation we would have a cubical field of view with detector plates forming the lateral faces of the cubical field of view(Figure 8). With the current apparatus, we put together a setup with a field of view similar to a plus(+)-shaped prism. The setup is shown in Figure 9 and 10.

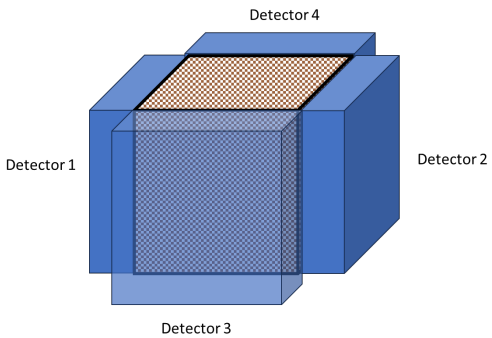

Figure 8: Ideal Setup

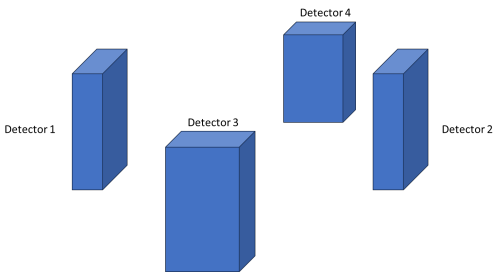

Figure 9: Depiction of the proposed setup

For the purpose of data collection, we used a setup with a distance of 268 mm between the opposite plates. Each of the detector plates were of the size 50 mm $\times$ 50 mm.

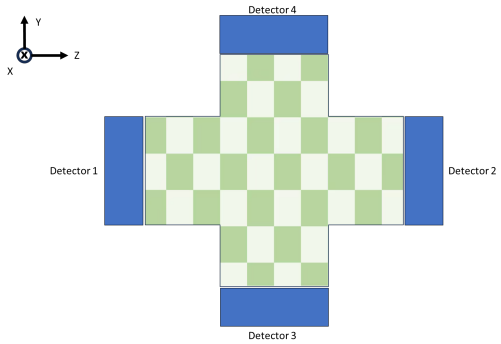

Figure 10: Top View of the Field of View of proposed setup

7 Results for the New Setup

The results indicate that the proposed setup improves upon the precision of detection over the initial setup. Although, the x direction histogram is similar to what we obtained with the initial setup. Along the y and z axes, a strong peak in the histogram is seen predicting the position of the source. Since we have introduced discretization, the precision is bounded by the size of a discretized block i.e. by 1 mm, hence we report the Full Width at Half Maximum(FWHM) as < 1 mm.

X-coordinate	Mean	FWHM
Intersection Estimate	-0.0499	4.2300
Iteration 1	0.0692	4.9138
Iteration 2	0.1283	5.1288
Iteration 3	0.1507	5.1904
Iteration 4	0.1639	5.1465
Iteration 5	0.1918	5.0995

Y-coordinate	Mean	FWHM
Intersection Estimate	1.7857	5.4191
Iteration 1	0.5000	≤ 1
Iteration 2	0.5000	≤ 1
Iteration 3	0.5000	≤ 1
Iteration 4	0.5000	≤ 1
Iteration 5	0.5000	≤ 1

Z-coordinate	Mean	FWHM
Intersection Estimate	1.3040	6.7689
Iteration 1	0.5000	≤ 1
Iteration 2	0.5000	≤ 1
Iteration 3	0.5000	≤ 1
Iteration 4	0.5000	≤ 1
Iteration 5	0.5000	≤ 1

Table 4: Results for Proposed Setup (in mm)

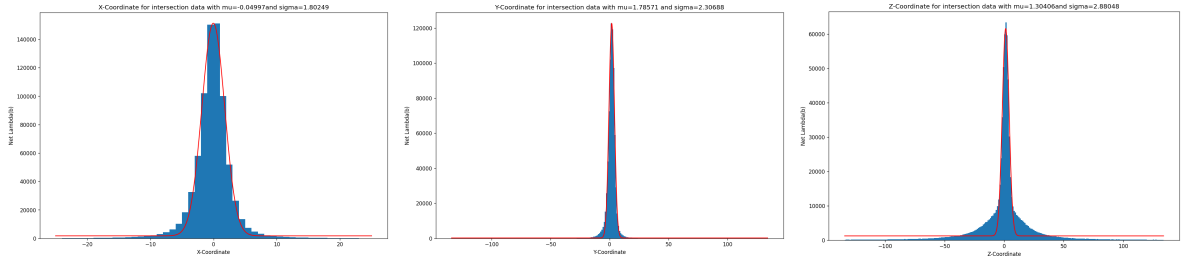

Figure 11: Intersection plots for Proposed Setup

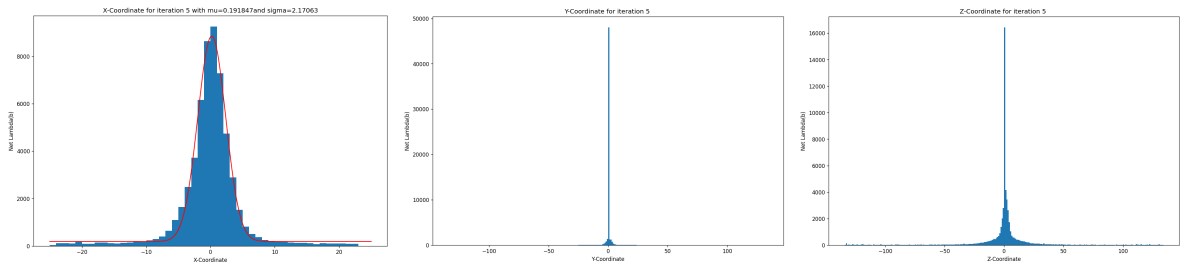

Figure 12: MLEM Iteration 5 plots for Proposed Setup

8 Future Possible Work

An analysis of the resolution of the current setup can be carried out by placing multiple sources in the field of view. Further analysis of how many iterations of the MLEM algorithm are optimal for a given dataset can be carried out.

9 Possible Applications

The proposed setup with the MLEM algorithm can be used for applications in the PET of small animals and for scanning tumors in specific parts of human body such as breast cancer etc.

References

[1] Biswajit Das et al. "Development of a GAGG (Ce)-based compact 3D scanning setup for assessment of active volume in γ-ray detectors". In: *Nuclear Instruments and Methods in Physics Research Section A: Accelerators, Spectrometers, Detectors and Associated Equipment* 1048 (2023), p. 167928.

[2] A. P. Dempster, N. M. Laird, and D. B. Rubin. "Maximum Likelihood from Incomplete Data via the EM Algorithm". In: *Journal of the Royal Statistical Society. Series B (Methodological)* 39.1 (1977), pp. 1–38. ISSN: 00359246. URL: `http://www.jstor.org/stable/2984875` (visited on 06/24/2025).

[3] *Results of the computations and relevant code used for preparing the report.* `https://github.com/adi0ga/GRI`.

[4] L. A. Shepp and Y. Vardi. "Maximum Likelihood Reconstruction for Emission Tomography". In: *IEEE Transactions on Medical Imaging* 1.2 (1982), pp. 113–122. DOI: `10.1109/TMI.1982.4307558`.